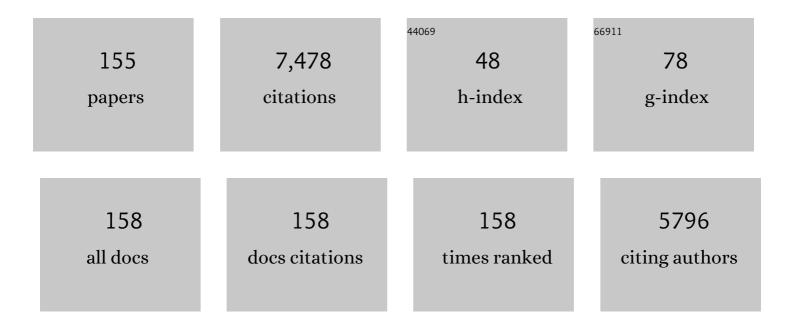
List of Publications by Year in descending order

Source: https://exaly.com/author-pdf/9485674/publications.pdf Version: 2024-02-01



#	Article	IF	CITATIONS
1	Highâ€Purity Inorganic Perovskite Films for Solar Cells with 9.72 % Efficiency. Angewandte Chemie - International Edition, 2018, 57, 3787-3791.	13.8	404
2	Lanthanide Ions Doped CsPbBr <sub>3</sub> Halides for HTMâ€Free 10.14%â€Efficiency Inorganic Perovskite Solar Cell with an Ultrahigh Openâ€Circuit Voltage of 1.594 V. Advanced Energy Materials, 2018, 8, 1802346.	19.5	387
3	Transparent Metal Selenide Alloy Counter Electrodes for Highâ€Efficiency Bifacial Dyeâ€Sensitized Solar Cells. Angewandte Chemie - International Edition, 2014, 53, 14569-14574.	13.8	231
4	Platinumâ€Free Binary Coâ€Ni Alloy Counter Electrodes for Efficient Dyeâ€Sensitized Solar Cells. Angewandte Chemie - International Edition, 2014, 53, 10799-10803.	13.8	205
5	Asymmetric Trilayer Allâ€Polymer Dielectric Composites with Simultaneous High Efficiency and High Energy Density: A Novel Design Targeting Advanced Energy Storage Capacitors. Advanced Functional Materials, 2021, 31, 2100280.	14.9	179
6	Dissolution Engineering of Platinum Alloy Counter Electrodes in Dyeâ€Sensitized Solar Cells. Angewandte Chemie - International Edition, 2015, 54, 11448-11452.	13.8	168
7	Recent advances in critical materials for quantum dot-sensitized solar cells: a review. Journal of Materials Chemistry A, 2015, 3, 17497-17510.	10.3	158
8	Rapid Conversion from Carbohydrates to Large-Scale Carbon Quantum Dots for All-Weather Solar Cells. ACS Nano, 2017, 11, 1540-1547.	14.6	155
9	Lattice Modulation of Alkali Metal Cations Doped Cs <sub>1â^'<i>x</i></sub> R <i><sub>x</sub></i> PbBr <sub>3</sub> Halides for Inorganic Perovskite Solar Cells. Solar Rrl, 2018, 2, 1800164.	5.8	154
10	Interface Engineering of Imidazolium Ionic Liquids toward Efficient and Stable CsPbBr <sub>3</sub> Perovskite Solar Cells. ACS Applied Materials & Interfaces, 2020, 12, 4540-4548.	8.0	132
11	Transparent nickel selenide alloy counter electrodes for bifacial dye-sensitized solar cells exceeding 10% efficiency. Nanoscale, 2014, 6, 12601-12608.	5.6	124
12	Robust electrocatalysts from an alloyed Pt–Ru–M (M = Cr, Fe, Co, Ni, Mo)-decorated Ti mesh for hydrogen evolution by seawater splitting. Journal of Materials Chemistry A, 2016, 4, 6513-6520.	10.3	118
13	Simplified Perovskite Solar Cell with 4.1% Efficiency Employing Inorganic CsPbBr <sub>3</sub> as Light Absorber. Small, 2018, 14, e1704443.	10.0	113
14	Carbonâ€Electrodeâ€Tailored Allâ€Inorganic Perovskite Solar Cells To Harvest Solar and Waterâ€Vapor Energy. Angewandte Chemie - International Edition, 2018, 57, 5746-5749.	13.8	112
15	9.13%-Efficiency and stable inorganic CsPbBr3 solar cells. Lead-free CsSnBr3-xlx quantum dots promote charge extraction. Journal of Power Sources, 2018, 399, 76-82.	7.8	105
16	Recent advances in alloy counter electrodes for dye-sensitized solar cells. A critical review. Electrochimica Acta, 2015, 178, 886-899.	5.2	104
17	Efficient dye-sensitized solar cells from polyaniline–single wall carbon nanotube complex counter electrodes. Journal of Materials Chemistry A, 2014, 2, 3119.	10.3	103
18	Highâ€Purity Inorganic Perovskite Films for Solar Cells with 9.72 % Efficiency. Angewandte Chemie, 2018, 130, 3849-3853.	2.0	99

#	Article	IF	CITATIONS
19	Low-Cost Counter Electrodes From CoPt Alloys For Efficient Dye-Sensitized Solar Cells. ACS Applied Materials & Interfaces, 2014, 6, 4812-4818.	8.0	96
20	A Solar Cell That Is Triggered by Sun and Rain. Angewandte Chemie - International Edition, 2016, 55, 5243-5246.	13.8	96
21	Poly(3-hexylthiophene)/zinc phthalocyanine composites for advanced interface engineering of 10.03%-efficiency CsPbBr <sub>3</sub> perovskite solar cells. Journal of Materials Chemistry A, 2019, 7, 12635-12644.	10.3	94
22	Achieving Concurrent High Energy Density and Efficiency in All-Polymer Layered Paraelectric/Ferroelectric Composites via Introducing a Moderate Layer. ACS Applied Materials & Interfaces, 2021, 13, 27522-27532.	8.0	87
23	Rapid charge-transfer in polypyrrole–single wall carbon nanotube complex counter electrodes: Improved photovoltaic performances of dye-sensitized solar cells. Journal of Power Sources, 2014, 256, 170-177.	7.8	86
24	Using SnO <sub>2</sub> QDs and CsMBr <sub>3</sub> (M = Sn, Bi, Cu) QDs as Chargeâ€Transporting Materials for 10.6%â€Efficiency Allâ€Inorganic CsPbBr <sub>3</sub> Perovskite Solar Cells with an Ultrahigh Openâ€Circuit Voltage of 1.610 V. Solar Rrl, 2019, 3, 1800284.	5.8	84
25	Toward efficient and air-stable carbon-based all-inorganic perovskite solar cells through substituting CsPbBr3 films with transition metal ions. Chemical Engineering Journal, 2019, 375, 121930.	12.7	82
26	Mesoporous TiO2 anodes for efficient dye-sensitized solar cells: An efficiency of 9.86% under one sun illumination. Journal of Power Sources, 2014, 267, 445-451.	7.8	74
27	Complexation of polyaniline and graphene for efficient counter electrodes in dye-sensitized solar cells: Enhanced charge transfer ability. Journal of Power Sources, 2014, 256, 8-13.	7.8	71
28	Quasi-solid-state dye-sensitized solar cell from polyaniline integrated poly(hexamethylene) Tj ETQq0 0 0 rgBT /Ove 5326.	erlock 10 <sup>-</sup> 10.3	Tf 50 387 Td 66
29	PtRu nanofiber alloy counter electrodes for dye-sensitized solar cells. Journal of Power Sources, 2014, 258, 117-121.	7.8	66
30	Robust Polyaniline–Graphene Complex Counter Electrodes For Efficient Dye-Sensitized Solar Cells. ACS Applied Materials & Interfaces, 2014, 6, 8230-8236.	8.0	66
31	An all-weather solar cell that can harvest energy from sunlight and rain. Nano Energy, 2016, 30, 818-824.	16.0	65
32	Enhanced photovoltaic performances of quasi-solid-state dye-sensitized solar cells using a novel conducting gel electrolyte. Journal of Power Sources, 2014, 248, 923-930.	7.8	64
33	Low-cost CoPt alloy counter electrodes for efficient dye-sensitized solar cells. Journal of Power Sources, 2014, 260, 180-185.	7.8	63
34	Alloy ontrolled Work Function for Enhanced Charge Extraction in Allâ€Inorganic CsPbBr <sub>3</sub> Perovskite Solar Cells. ChemSusChem, 2018, 11, 1432-1437.	6.8	62
35	Enhanced Efficiency of Air-Stable CsPbBr <sub>3</sub> Perovskite Solar Cells by Defect Dual Passivation and Grain Size Enlargement with a Multifunctional Additive. ACS Applied Materials & Interfaces, 2020, 12, 36092-36101.	8.0	62
36	Grain Enlargement and Defect Passivation with Melamine Additives for High Efficiency and Stable CsPbBr <sub>3</sub> Perovskite Solar Cells. ChemSusChem, 2020, 13, 1834-1843.	6.8	62

#	Article	IF	CITATIONS
37	Efficient quasi-solid-state dye-sensitized solar cells from graphene incorporated conducting gel electrolytes. Journal of Materials Chemistry A, 2014, 2, 2814.	10.3	60
38	Efficient quasi-solid-state dye-sensitized solar cells employing polyaniline and polypyrrole incorporated microporous conducting gel electrolytes. Journal of Power Sources, 2014, 254, 98-105.	7.8	59
39	Imbibition of polypyrrole into three-dimensional poly(hydroxyethyl methacrylate/glycerol) gel electrolyte for robust quasi-solid-state dye-sensitized solar cells. Journal of Materials Chemistry A, 2013, 1, 8055.	10.3	57
40	Spray-assisted deposition of CsPbBr3 films in ambient air for large-area inorganic perovskite solar cells. Materials Today Energy, 2018, 10, 146-152.	4.7	57
41	Universal Dynamic Liquid Interface for Healing Perovskite Solar Cells. Advanced Materials, 2022, 34, e2202301.	21.0	57
42	Multifunctional graphene incorporated conducting gel electrolytes in enhancing photovoltaic performances of quasi-solid-state dye-sensitized solar cells. Journal of Power Sources, 2014, 260, 225-232.	7.8	56
43	Photoelectric conversion beyond sunny days: all-weather carbon quantum dot solar cells. Journal of Materials Chemistry A, 2017, 5, 2143-2150.	10.3	54
44	Solid-state dye-sensitized solar cells from poly(ethylene oxide)/polyaniline electrolytes with catalytic and hole-transporting characteristics. Journal of Materials Chemistry A, 2015, 3, 5368-5374.	10.3	53
45	Biomass converted carbon quantum dots for all-weather solar cells. Electrochimica Acta, 2017, 257, 259-266.	5.2	53
46	Transmission enhanced photoanodes for efficient dye-sensitized solar cells. Electrochimica Acta, 2014, 125, 646-651.	5.2	52
47	Advanced Modification of Perovskite Surfaces for Defect Passivation and Efficient Charge Extraction in Air-Stable CsPbBr <sub>3</sub> Perovskite Solar Cells. ACS Sustainable Chemistry and Engineering, 2019, 7, 19286-19294.	6.7	51
48	Platinum Alloy Tailored Allâ€Weather Solar Cells for Energy Harvesting from Sun and Rain. Angewandte Chemie - International Edition, 2016, 55, 14412-14416.	13.8	49
49	Enhanced charge extraction by setting intermediate energy levels in all-inorganic CsPbBr3 perovskite solar cells. Electrochimica Acta, 2018, 279, 84-90.	5.2	49
50	Enhanced dye illumination in dye-sensitized solar cells using TiO <sub>2</sub> /GeO <sub>2</sub> photo-anodes. Journal of Materials Chemistry A, 2014, 2, 12459.	10.3	48
51	Cost-effective, transparent iron selenide nanoporous alloy counter electrode for bifacial dye-sensitized solar cell. Journal of Power Sources, 2015, 282, 79-86.	7.8	47
52	Bifacial dye-sensitized solar cells with enhanced rear efficiency and power output. Nanoscale, 2014, 6, 15127-15133.	5.6	45
53	Employment of ionic liquid-imbibed polymer gel electrolyte for efficient quasi-solid-state dye-sensitized solar cells. Journal of Power Sources, 2014, 248, 816-821.	7.8	44
54	Bifacial dye-sensitized solar cells with transparent cobalt selenide alloy counter electrodes. Journal of Power Sources, 2015, 284, 349-354.	7.8	44

#	Article	IF	CITATIONS
55	Enhanced energy level alignment and hole extraction of carbon electrode for air-stable hole-transporting material-free CsPbBr3 perovskite solar cells. Solar Energy Materials and Solar Cells, 2020, 205, 110267.	6.2	43
56	Enhanced photocatalytic activity from Gd, La codoped TiO2 nanotube array photocatalysts under visible-light irradiation. Applied Surface Science, 2013, 284, 837-842.	6.1	42
57	Efficient In2S3 Quantum dotâ^'sensitized Solar Cells: A Promising Power Conversion Efficiency of 1.30%. Electrochimica Acta, 2014, 139, 381-385.	5.2	42
58	Platinum-free binary Fe–Co nanofiber alloy counter electrodes for dye-sensitized solar cells. Journal of Power Sources, 2014, 268, 56-62.	7.8	42
59	Bifacial dye-sensitized solar cells from covalent-bonded polyaniline–multiwalled carbon nanotube complex counter electrodes. Journal of Power Sources, 2015, 275, 489-497.	7.8	42
60	Improved charge extraction through interface engineering for 10.12% efficiency and stable CsPbBr <sub>3</sub> perovskite solar cells. Journal of Materials Chemistry A, 2020, 8, 20987-20997.	10.3	42
61	Multifunctional graphene incorporated polyacrylamide conducting gel electrolytes for efficient quasi-solid-state quantum dot-sensitized solar cells. Journal of Power Sources, 2015, 284, 369-376.	7.8	40
62	Can dye-sensitized solar cells generate electricity in the dark?. Nano Energy, 2017, 33, 266-271.	16.0	40
63	Transmission booster from SiO2 incorporated TiO2 crystallites: Enhanced conversion efficiency in dye-sensitized solar cells. Electrochimica Acta, 2014, 134, 281-286.	5.2	39
64	Graphene enabled all-weather solar cells for electricity harvest from sun and rain. Journal of Materials Chemistry A, 2016, 4, 13235-13241.	10.3	38
65	A simple approach of enhancing photovoltaic performances of quasi-solid-state dye-sensitized solar cells by integrating conducting polyaniline into electrical insulating gel electrolyte. Journal of Power Sources, 2014, 245, 468-474.	7.8	37
66	Hydrogen-Bonded Dopant-Free Hole Transport Material Enables Efficient and Stable Inverted Perovskite Solar Cells. CCS Chemistry, 2022, 4, 3084-3094.	7.8	37
67	Full-ionic liquid gel electrolytes: Enhanced photovoltaic performances in dye-sensitized solar cells. Journal of Power Sources, 2014, 264, 83-91.	7.8	36
68	Conducting gel electrolytes with microporous structures for efficient quasi-solid-state dye-sensitized solar cells. Journal of Power Sources, 2015, 273, 1148-1155.	7.8	36
69	Titanium dioxide/calcium fluoride nanocrystallite for efficient dye-sensitized solar cell. A strategy of enhancing light harvest. Journal of Power Sources, 2015, 275, 175-180.	7.8	35
70	Transparent molybdenum sulfide decorated polyaniline complex counter electrodes for efficient bifacial dye-sensitized solar cells. Solar Energy, 2017, 147, 470-478.	6.1	35
71	A ceramic NiO/ZrO2 separator for high-temperature supercapacitor up to 140â€ <sup>-</sup> °C. Journal of Power Sources, 2018, 400, 126-134.	7.8	34
72	Co/Se and Ni/Se nanocomposite films prepared by magnetron sputtering as counter electrodes for dye-sensitized solar cells. Solar Energy, 2019, 180, 85-91.	6.1	34

#	Article	IF	CITATIONS
73	Carbide decorated carbon nanotube electrocatalyst for high-efficiency hydrogen evolution from seawater. RSC Advances, 2016, 6, 93267-93274.	3.6	33
74	Sonochemistry-assisted black/red phosphorus hybrid quantum dots for dye-sensitized solar cells. Journal of Power Sources, 2019, 410-411, 53-58.	7.8	33
75	Counter electrodes from binary ruthenium selenide alloys for dye-sensitized solar cells. Journal of Power Sources, 2014, 271, 108-113.	7.8	32
76	Counter electrodes from polyanilineâ^'carbon nanotube complex/graphene oxide multilayers for dye-sensitized solar cell application. Electrochimica Acta, 2014, 125, 510-515.	5.2	32
77	Efficient interface engineering of N, N'-Dicyclohexylcarbodiimide for stable HTMs-free CsPbBr3 perovskite solar cells with 10.16%-efficiency. Chemical Engineering Journal, 2022, 428, 131950.	12.7	32
78	Reducing Energy Disorder for Efficient and Stable Snâ^'Pb Alloyed Perovskite Solar Cells Angewandte Chemie - International Edition, 2022, 61, .	13.8	32
79	Self-assembly of graphene oxide/polyaniline multilayer counter electrodes for efficient dye-sensitized solar cells. Electrochimica Acta, 2014, 121, 136-142.	5.2	30
80	Enhanced charge extraction in carbon-based all-inorganic CsPbBr3 perovskite solar cells by dual-function interface engineering. Electrochimica Acta, 2019, 328, 135102.	5.2	30
81	Counter electrodes from polyanilineâ^'graphene complex/graphene oxide multilayers for dyeâ^'sensitized solar cells. Electrochimica Acta, 2014, 137, 175-182.	5.2	29
82	Costâ^'effective alloy counter electrodes as a new avenue for highâ^'efficiency dyeâ^'sensitized solar cells. Electrochimica Acta, 2015, 158, 397-402.	5.2	29
83	Ultraviolet filtration and defect passivation for efficient and photostable CsPbBr3 perovskite solar cells by interface engineering with ultraviolet absorber. Chemical Engineering Journal, 2021, 404, 126548.	12.7	29
84	Enhanced charge extraction with all-carbon electrodes for inorganic CsPbBr <sub>3</sub> perovskite solar cells. Dalton Transactions, 2018, 47, 15283-15287.	3.3	28
85	Efficiency enhancement of bifacial dye-sensitized solar cells through bi-tandem carbon quantum dots tailored transparent counter electrodes. Electrochimica Acta, 2018, 278, 204-209.	5.2	28
86	Multifunctional brominated graphene oxide boosted charge extraction for high-efficiency and stable all-inorganic CsPbBr3 perovskite solar cells. Chemical Engineering Journal, 2021, 412, 128727.	12.7	28
87	Robust conducting gel electrolytes for efficient quasi-solid-state dye-sensitized solar cells. Electrochimica Acta, 2014, 137, 57-64.	5.2	27
88	7.35% Efficiency rear-irradiated flexible dye-sensitized solar cells by sealing liquid electrolyte in a groove. Chemical Communications, 2015, 51, 491-494.	4.1	27
89	Boosted hole extraction in all-inorganic CsPbBr3 perovskite solar cells by interface engineering using MoO2/N-doped carbon nanospheres composite. Solar Energy Materials and Solar Cells, 2020, 209, 110460.	6.2	27
90	Phase Control of Csâ€Pbâ€Br Derivatives to Suppress 0D Cs <sub>4</sub> PbBr <sub>6</sub> for Highâ€Efficiency and Stable Allâ€Inorganic CsPbBr <sub>3</sub> Perovskite Solar Cells. Small, 2022, 18, e2106323.	10.0	27

#	Article	IF	CITATIONS
91	Cubic carbon quantum dots for light-harvesters in mesoscopic solar cells. Electrochimica Acta, 2018, 275, 275-280.	5.2	26
92	A porous ceramic membrane tailored high-temperature supercapacitor. Journal of Power Sources, 2018, 379, 60-67.	7.8	26
93	Compositional Engineering of Chloride Ionâ€Doped CsPbBr 3 Halides for Highly Efficient and Stable Allâ€Inorganic Perovskite Solar Cells. Solar Rrl, 2020, 4, 2000362.	5.8	26
94	A "double-sided tape―modifier bridging the TiO <sub>2</sub> /perovskite buried interface for efficient and stable all-inorganic perovskite solar cells. Journal of Materials Chemistry A, 2022, 10, 6649-6661.	10.3	25
95	Dimensionality Control of SnO <sub>2</sub> Films for Hysteresis-Free, All-Inorganic CsPbBr <sub>3</sub> Perovskite Solar Cells with Efficiency Exceeding 10%. ACS Applied Materials & Interfaces, 2021, 13, 11058-11066.	8.0	24
96	Multifunctional interface modifier ammonium silicofluoride for efficient and stable all-inorganic CsPbBr3 perovskite solar cells. Chemical Engineering Journal, 2022, 431, 134193.	12.7	24
97	A dye-sensitized solar cell having polyaniline species in each component with 3.1%-efficiency. Journal of Power Sources, 2015, 284, 178-185.	7.8	23
98	Insights of close contact between polyaniline and FTO substrate for enhanced photovoltaic performances of dye-sensitized solar cells. Electrochimica Acta, 2014, 125, 163-169.	5.2	22
99	A Solar Cell That Is Triggered by Sun and Rain. Angewandte Chemie, 2016, 128, 5329-5332.	2.0	22
100	Dissolution-resistant platinum alloy counter electrodes for stable dye-sensitized solar cells. Electrochimica Acta, 2016, 190, 409-418.	5.2	22
101	Harvest rain energy by polyaniline-graphene composite films. Renewable Energy, 2018, 125, 995-1002.	8.9	22
102	Transparent ternary alloy counter electrodes for high-efficiency bifacial dye-sensitized solar cells. Solar Energy, 2018, 170, 762-768.	6.1	22
103	Incorporation of H3PO4 into three-dimensional polyacrylamide-graft-starch hydrogel frameworks for robust high-temperature proton exchange membrane fuel cells. International Journal of Hydrogen Energy, 2014, 39, 4447-4458.	7.1	21
104	Counter electrodes from polymorphic platinum-nickel hollow alloys for high-efficiency dye-sensitized solar cells. Journal of Power Sources, 2016, 328, 185-194.	7.8	21
105	H3PO4 imbibed polyacrylamide-graft-chitosan frameworks for high-temperature proton exchange membranes. Journal of Power Sources, 2014, 249, 277-284.	7.8	20
106	Bifacial quantum dot-sensitized solar cells with transparent cobalt selenide counter electrodes. Journal of Power Sources, 2015, 278, 183-189.	7.8	19
107	Long persistence phosphor assisted all-weather solar cells. Electricity generation beyond sunny days. Chemical Communications, 2017, 53, 3209-3212.	4.1	19
108	Robust electrocatalysts from metal doped W <sub>18</sub> O <sub>49</sub> nanofibers for hydrogen evolution. Chemical Communications, 2017, 53, 4323-4326.	4.1	19

#	Article	IF	CITATIONS
109	Carbonâ€Electrodeâ€Tailored Allâ€Inorganic Perovskite Solar Cells To Harvest Solar and Waterâ€Vapor Energy. Angewandte Chemie, 2018, 130, 5848-5851.	2.0	19

## Quasi-solid-state dye-sensitized solar cells from hydrophobic poly(hydroxyethyl) Tj ETQq0 0 0 rgBT /Overlock 10 Tf $\frac{50}{4.0}$ 702 Td (methacry $\frac{110}{18}$

111	Solid-state electrolytes from polysulfide integrated polyvinylpyrrolidone for quantum dot-sensitized solar cells. RSC Advances, 2014, 4, 60478-60483.	3.6	18
112	Efficient dye-sensitized solar cells from curved silicate microsheet caged TiO 2 photoanodes. An avenue of enhancing light harvesting. Electrochimica Acta, 2015, 178, 18-24.	5.2	18
113	An avenue of sealing liquid electrolyte in flexible dye-sensitized solar cells. Journal of Power Sources, 2015, 274, 304-309.	7.8	18
114	Platinum alloy decorated polyaniline counter electrodes for dye-sensitized solar cells. Electrochimica Acta, 2016, 190, 76-84.	5.2	18
115	All-solid-state quantum dot-sensitized solar cell from plastic crystal electrolyte. RSC Advances, 2015, 5, 33463-33467.	3.6	17
116	Alloying of platinum and molybdenum for transparent counter electrodes. A strategy of enhancing power output for bifacial dye-sensitized solar cells. RSC Advances, 2015, 5, 51600-51607.	3.6	16
117	Counter electrode electrocatalysts from binary Pd–Co alloy nanoparticles for dye-sensitized solar cells. Solar Energy, 2016, 124, 68-75.	6.1	15
118	Mo incorporated W 18 O 49 nanofibers as robust electrocatalysts for high-efficiency hydrogen evolution. International Journal of Hydrogen Energy, 2017, 42, 14534-14546.	7.1	15
119	Three-dimensional hydrogel frameworks for high-temperature proton exchange membrane fuel cells. Journal of Materials Science, 2014, 49, 5481-5491.	3.7	14
120	Enhanced hole extraction by electron-rich alloys in all-inorganic CsPbBr <sub>3</sub> perovskite solar cells. Chemical Communications, 2021, 57, 7577-7580.	4.1	14
121	Cylindrical dye-sensitized solar cells with high efficiency and stability over time and incident angle. Chemical Communications, 2016, 52, 3528-3531.	4.1	13
122	Triâ€Brominated Perovskite Film Management and Multipleâ€Ionic Defect Passivation for Highly Efficient and Stable Solar Cells. Solar Rrl, 2021, 5, 2000819.	5.8	13
123	Efficient dye-sensitized solar cell from spiny polyaniline nanofiber counter electrode. Materials Letters, 2014, 119, 28-31.	2.6	12
124	Polypyrrole‑molybdenum sulfide complex as an efficient and transparent catalytic electrode for bifacial dye-sensitized solar cells. Catalysis Communications, 2022, 163, 106403.	3.3	12
125	Solar photocatalysts from Gd–La codoped TiO2 nanoparticles. Journal of Materials Science, 2014, 49, 3371-3378.	3.7	11
126	Poly(vinylidene fluoride)–implanted cobalt–platinum alloy counter electrodes for dye–sensitized solar cells. Electrochimica Acta, 2014, 147, 209-215.	5.2	11

#	Article	IF	CITATIONS
127	Bifunctional polyaniline electrode tailored hybridized solar cells for energy harvesting from sun and rain. Journal of Energy Chemistry, 2018, 27, 742-747.	12.9	11
128	EIS analysis of hydrophobic and hydrophilicTiO2 film. Electrochimica Acta, 2008, 54, 611-615.	5.2	10
129	Graphene-incorporated quasi-solid-state dye-sensitized solar cells. RSC Advances, 2015, 5, 43402-43407.	3.6	10
130	Platinum Alloy Tailored Allâ€Weather Solar Cells for Energy Harvesting from Sun and Rain. Angewandte Chemie, 2016, 128, 14624-14628.	2.0	10
131	ZnO nanorods assisted Ni1.1Pt and Co3.9Pt alloy microtube counter electrodes for efficient dye-sensitized solar cells. Electrochimica Acta, 2016, 190, 903-911.	5.2	10
132	Preparation and electrochemical properties of polyâ€2,5â€dihydroxyaniline/activated carbon composite electrode in organic electrolyte. Journal of Applied Polymer Science, 2013, 127, 4672-4680.	2.6	9
133	Interfacial engineering of hybridized solar cells for simultaneously harvesting solar and rain energies. Journal of Materials Chemistry A, 2017, 5, 18551-18560.	10.3	9
134	Self-powered flexible monoelectrodes from graphene/reduced graphene oxide composite films to harvest rain energy. Journal of Alloys and Compounds, 2019, 776, 31-35.	5.5	9
135	Application of poly(3,4-ethylenedioxythiophene):polystyrenesulfonate in polymer heterojunction solar cells. Journal of Materials Science, 2013, 48, 3528-3534.	3.7	8
136	Efficient Defect Passivation and Charge Extraction with Hexamethylenetetramine Interface Modification for Holeâ€Transporting Layersâ€Free CsPbBr <sub>3</sub> Perovskite Solar Cells. Solar Rrl, 2021, 5, 2100344.	5.8	8
137	Toward elevated light harvesting: efficient dye-sensitized solar cells with titanium dioxide/silica photoanodes. RSC Advances, 2015, 5, 46260-46266.	3.6	7
138	Room-temperature fabrication of multi-deformable perovskite solar cells made in a three-dimensional gel framework. RSC Advances, 2016, 6, 82933-82940.	3.6	7
139	Extra-high short-circuit current for bifacial solar cells in sunny and dark–light conditions. Chemical Communications, 2017, 53, 10046-10049.	4.1	7
140	Enhanced light harvesting of TiO2/La0.95Tb0.05PO4 photoanodes for dye-sensitized solar cells. Materials Chemistry and Physics, 2016, 173, 340-346.	4.0	6
141	Hybridized dye-sensitized solar cells for persistent power generation free of sun illumination. Electrochimica Acta, 2018, 280, 181-190.	5.2	6
142	Rain-responsive polypyrrole-graphene/PtCo electrodes for energy harvest. Electrochimica Acta, 2018, 285, 139-148.	5.2	6
143	Enhanced proton conductivity from phosphoric acidâ€incorporated 3D polyacrylamideâ€graftâ€starch hydrogel materials for highâ€ŧemperature proton exchange membranes. Journal of Applied Polymer Science, 2014, 131, .	2.6	5
144	Microporous gel electrolyte for quasi-solid-state dye-sensitized solar cell. Polymer Engineering and Science, 2014, 54, 2531-2535.	3.1	5

#	Article	IF	CITATIONS
145	Insights on the accumulation of charge carriers for enhanced electrical and photoelectric behaviors in conducting multilayer films. RSC Advances, 2013, 3, 25190.	3.6	3
146	An avenue of expanding triiodide reduction and shortening charge diffusion length in solid-state dye-sensitized solar cells. Journal of Power Sources, 2015, 273, 180-184.	7.8	3
147	Spatial confinement growth of perovskite nanocrystals for ultra-flexible solar cells. RSC Advances, 2016, 6, 59429-59437.	3.6	3
148	Reducing Energy Disorder for Efficient and Stable Snâ^'Pb Alloyed Perovskite Solar Cells Angewandte Chemie, 2022, 134, .	2.0	3
149	Preparation and electrochemical properties of polyaniline/α-RuCl <sub>3</sub> . <i>x</i> H <sub>2</sub> O composites for supercapacitor. Polymer Composites, 2013, 34, 2142-2147.	4.6	2
150	Corrosion behavior of anodic oxidized TiO2 film in seawater. Journal of Ocean University of China, 2010, 9, 376-380.	1.2	1
151	Growth of hexagonal polyaniline fibers with polyacrylamide pendants. Polymer Composites, 2014, 35, 253-262.	4.6	1
152	Insights on tunneled electrons for electrical and photoelectric behaviors in conducting multilayer films. Polymer Engineering and Science, 2015, 55, 107-112.	3.1	1
153	Selfâ€Powered Lowâ€Platinum Nanorod Alloy Monoelectrodes for Rain Energy Harvest. Energy Technology, 2018, 6, 1606-1609.	3.8	1
154	Using SnO2 QDs and CsMBr3 (M = Sn, Bi, Cu) QDs as Charge-Transporting Materials for 10.6%-Efficien All-Inorganic CsPbBr3 Perovskite Solar Cells with an Ultrahigh Open-Circuit Voltage of 1.610 V (Solar) Tj ETQq0		)verlock 10 T

Peculiar electrical and photoelectric behaviors in conducting multilayers: Insights into accumulative charge tunneling. Journal of Applied Polymer Science, 2014, 131, .